Universiteit Utrecht

Opleiding Natuur- en Sterrenkunde

Remote Viscosity Measurement of Acoustically Levitated Colloidal Droplets.

Bachelor Thesis

Milo Collaris

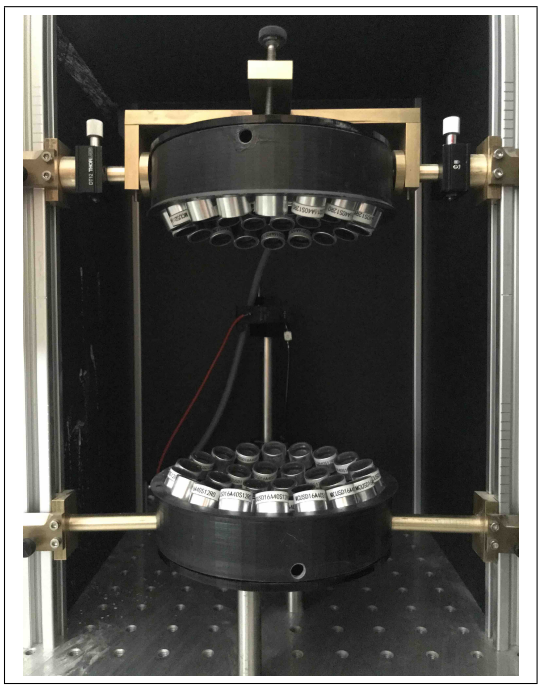

Supervisors:

Dr. S. Faez
Debye Institute

B. Yeroshenko MSc
Debye Institute

June 13, 2018

Abstract

Acoustic levitation makes it possible to remotely measure the viscosity of particles even if they have no electric or magnetic properties. This is done by acoustically levitating the droplet and measuring the damping constant of the resonant oscillation. To measure this the free decay method[1] is used where the droplet is excited into oscillation by turning the acoustic field off for 2.5 ms. After the excitation the damping of the oscillation is measured via stroboscopic imaging, using the shutter of a camera and calculating the radius of the droplet by fitting an ellipse to the edge of the droplet. Water and colloidal droplets with 1 μm particles based on polymethacrylate are investigated and since the droplets evaporate in the acoustic levitator an increase in viscosity is measured for the colloidal droplet that eventually crystallizes.

Contents

1 Introduction

The study of dynamic properties of liquid droplets is of great interest to scientist for a better understanding of the characteristics and possible industrial applications of materials. Measurement of properties such as surface tension and viscosity can be difficult since the droplet is in contact with a surface, which can result in unwanted frictions and contamination of the droplet. Acoustic levitation is a method to let particles or liquid droplets float in an ultrasonic acoustic field, where before this was only possible for particles with magnetic or electric components via the use of a magnetic or electric field. Using this method contactless measurements can be done. In this thesis, the floating droplets are trapped in the central node of the acoustic field, constructed of two plates filled with ultrasonic transducers. The shape of the droplet and especially the damping of the resonant oscillation after an excitation is investigated.

As Kremer *et al.*[1] discussed, there are two methods to excite droplets into oscillation, a steady-state frequency response (FRF) and a free decay (FD) method. The former uses an increasing modulation frequency while the droplet's response is monitored continuously and the latter initially excites the droplet into oscillation and after the excitation the decaying oscillation is recorded.[1] In this thesis the FD method is used and for excitation the acoustic field is briefly turned off, in the order of ms. This way the droplet is in free fall until the field is turned back on, ceasing the excitation, the droplet is dragged back into the central node.

The damping of the oscillation and thus the reduction of the change in radius of the ellipsoidal droplet is linked to the viscosity of the droplet. So with the acoustic levitator the viscosity can be measured remotely. Also the droplet is evaporating inside the trap which results in a changing damping constant for the oscillation. The goal of this thesis is to investigate a droplet of colloidal suspension and measure the viscosity while evaporating. The hypothesis is that while evaporating the viscosity increases and that a change in phase becomes visible due to crystallization of the droplet.

This thesis starts with a theoretical framework for free oscillating droplets and the relation between the damping of the resonant oscillation and the viscosity of the droplet. Then the experimental setup will be explained and the methods to analyze the data will be discussed. Afterwards the data will be analyzed and the results will be presented and discussed. Finally the conclusions are stated and an outlook for further research will be given.

2 Theory

In this section the theoretical framework for droplets in an acoustic field will be described. First the basic principles of the acoustic field will be explained. Then the relation between the viscosity and the damping of the resonant oscillation will be derived, following the calculations of H. Lamb's Hydrodynamics[2]. Afterwards the mathematics of ellipses will be discussed and finally a model from where the damping constant can be derived will be presented.

2.1 Acoustic field

A levitated droplet in an acoustic field is subject to two forces: the axial force along the axis of levitation, which is responsible for the droplet not falling down, and the radial force perpendicular to the axis of levitation. The ratio of these forces are (5:1) resulting in an ellipsoidal shape of the droplet.[1] Further theoretical background of the forces that play a role in acoustically levitating droplets and the boundaries of this system are beyond the scope of this thesis.

Inside the acoustic trap standing waves will form with a layer pattern of nodes. These nodes typically form every $\frac{1}{2}\lambda$. For a sound velocity of $v_{sound} = 343\ m \cdot s^{-1}$ at room temperature and a frequency of $f = 40$ kHz the spatial separation of the nodes of the standing wave becomes:

$$\frac{1}{2}\lambda = \frac{v_{sound}}{2f} = \frac{343}{2 * 40 * 10^3} = 4.29mm.$$

2.2 Viscosity

In this section the relation between the damping constant τ (in s) and dynamic viscosity μ (in $Pa \cdot s$) will be derived. Viscosity is a measure of the resistance of a fluid to deformation under shear stress. Viscous forces oppose the motion of one portion of a fluid relative to another.[3, p. 431]. The derivation starts from the relation between the change in total energy and dissipation, which is the lost of mechanical energy[3, p. 246], given by H. Lamb equation (10) from article 355:[1]

$$\frac{d}{dt}(T + V) = -2F_{av}, \tag{1}$$

with T and V the kinetic and potential energy respectively and F_{av} the average dissipation. First the dissipation F will be derived, followed by the kinetic and potential energy T and V to eventually get an expression for viscosity as a function of the damping constant from equation (1). The dissipation F is given by Lamb(6) using an irrotational approximation:

$$2F = \mu \iint \frac{\partial q^2}{\partial r} r^2 d\omega = \mu r^2 \frac{\partial}{\partial r} \iint q^2 d\omega. \tag{2}$$

[1] The following calculations follow the reasoning of article 355 of H. Lamb. The equations from H. Lamb will simply be referred to as Lamb(10).

Where q is a velocity term[3, p. 595], r is the radius of the droplet and ω is a frequency term. Using a relation for q and the velocity potential ϕ gives the following identity:

$$r^2 \iint q^2 d\omega = \frac{\partial}{\partial r} \iint \phi \frac{\partial \phi}{\partial r} r^2 d\omega. \tag{3}$$

Here the velocity potential can be expressed as a function of radius and time:

$$\phi = A \frac{r^n}{a^n} S_n \cos(\sigma t + \epsilon). \tag{4}$$

With A and ϵ arbitrary constants, a the radius in the undisturbed state[3, p. 443], S_n a surface harmonic, $\sigma/2\pi$ a frequency[3, p. 241] and n an integer representing modes of oscillation.

From equations (2), (3) and (4) it can be calculated, as is shown in Appendix A.1, that the average dissipation F_{av} is given by:

$$2F_{av} = n(2n+1)(n-1)\frac{\mu}{a} \iint S_n^2 d\omega A^2. \tag{5}$$

Now for the determination of the potential and kinetic energy H. Lamb uses that twice the kinetic energy is given by:[3, p. 445]

$$2T = \rho \iint \phi \frac{\partial \phi}{\partial r} r^2 d\omega = \rho n a \Big(\frac{r}{a}\Big)^{2n+1} \iint S_n^2 d\omega A^2 \cos^2(\sigma t + \epsilon), \tag{6}$$

with ρ the density of the droplet. On average half of the total energy will be for the kinetic energy T and half for the potential energy V. The potential energy will be defined with a $\sin^2(\sigma t + \epsilon)$ for the right exchange between the energies:

$$T = \frac{1}{2}\rho n a \Big(\frac{r}{a}\Big)^{2n+1} \iint S_n^2 d\omega A^2 \cos^2(\sigma t + \epsilon),$$
$$V = \frac{1}{2}\rho n a \Big(\frac{r}{a}\Big)^{2n+1} \iint S_n^2 d\omega A^2 \sin^2(\sigma t + \epsilon).$$

Combining these and the identity $\cos^2(x) + \sin^2(x) = 1$ gives the sum:

$$T + V = \frac{1}{2}\rho n a \Big(\frac{r}{a}\Big)^{2n+1} \iint S_n^2 d\omega A^2 \tag{7}$$

Now as last step filling in the expressions for F_{av}, equation (5), and $T + V$, equation (7), in equation (1) it can be derived, as shown in Appendix A.2, that for the viscosity μ it holds that:

$$\mu = \frac{\rho a^2}{\tau(n-1)(2n+1)}.^2 \tag{8}$$

The mode of interest for the viscosity determination is the $n = 2$ mode since $n = 0$ and $n = 1$ represent respectively the volumetric pulsation and the translatory motion of the droplet.[5]

[2]This formula is also used by Kremer *et al.*[1], Langstaff *et al.*[4] and Becker *et al.*[5] for viscosity measurement of acoustically levitated droplets.

This equation, according to Prosperetti *et al.* is only valid for drops with Ohnesorge number smaller than 0.1. The Ohnesorge number is given by:[6]

$$Oh = \frac{\mu}{\sqrt{\rho\sigma a}} \tag{9}$$

A calculation for a water droplet with $\rho = 997\ Kg \cdot m^{-3}$, $\sigma = 71.97 \cdot 10^{-3}\ N \cdot m^{-1}$ and $\mu = 1.002 \cdot 10^{-3}\ Pa \cdot s$ gives a minimum volume equal spherical radius of $a = 1.40 \cdot 10^{-6}\ m = 14\ nm$. Which is several orders of magnitude smaller than the droplets that are levitated in this thesis, which have a radius in the order of mm.

2.3 Ellipse calculations

Since the data that is obtained is a two dimensional image of the ellipsoidal droplet, the calculations needed can be simplified to ellipses. The quadratic equation of an ellipse has the form:[3]

$$ax^2 + 2bxy + cy^2 + 2dx + 2fy + g = 0. \tag{10}$$

And from here it can be calculated that the radius of the droplet r, while considering a possible angle with the x-axis, is given by:

$$r = \sqrt{\frac{2(af^2 + cd^2 + gb^2 - 2bdf - acg)}{(b^2 - ac)(\pm\sqrt{(a-c)^2 + 4b} - (a+c))}}. \tag{11}$$

Where $\pm$ is used for calculating the horizontal and vertical radii respectively. This will be used to calculate the radius and the volume of the oscillating droplet inside the trap.

2.4 Damped harmonic oscillation

The damping of the resonant oscillation can be determined via the following formula for the radius $r(t)$ as function of time t:

$$r(t) = r_0 + Ae^{-\frac{t}{\tau}}cos(2\pi ft) + \xi. \tag{12}$$

In this formula the fitting parameters are the equilibrium radius of the drop r_0 in mm, the dimensionless amplitude of the drop shape oscillation A, the damping constant τ in s, the frequency f in Hz and ξ a noise factor. Because this noise factor can become large if the acoustic trap or the excitation method are not optimal another approach becomes helpful. Using the standard deviation of the radius of the droplet, the relation then becomes:

$$\begin{aligned}
\sigma_r^2 &= \langle r(t)^2 \rangle - \langle r(t) \rangle^2, \\
\sigma_r^2 &= r_0^2 + \xi^2 + \frac{1}{2}A^2 e^{\frac{2t}{\tau}} - r_0^2 - \xi^2, \\
\sigma_r &= \frac{1}{\sqrt{2}} A e^{\frac{t}{\tau}}.
\end{aligned} \tag{13}$$

[3]The calculations are from http://mathworld.wolfram.com/Ellipse.html. This is also used by Ben Hammel and Nick Sullivan-Molina in their Python class for ellipse fitting, which will be discussed in Data analysis, section 3.2.

3 Experiment

The viscosity of a droplet is dependent of the damping of its resonant oscillation. In order to have the droplet reach this resonant oscillation an excitation is needed. This can be done by the free decay method[1], where the droplet is excited into oscillation and after the excitation the damping of the oscillation is measured. The excitation is done by turning the field off for 2.5 ms to give the droplet a free fall. The time of the free fall is chosen so that whence the field is turned back on the droplet is caught back into the same node of the acoustic field. In order to derive the viscosity and the damping of the resonant frequency an analysis of the data is needed. This is done using Python and will be described in section 3.2.

3.1 Experimental setup

3.1.1 Acoustic levitator

The main part of the setup is the acoustic levitator which consists out of two panels, constructed as a cutout from a sphere with a radius of 110.5 mm. On these panels 72 transducers are installed with a sharp resonance at 40 kHz, all following the curvature of the panels.[4] For a view of the acoustic levitator see figure 1 and for a schematic overview of the setup see figure 2. The two panels are driven by a signal generator that outputs the 40 kHz block signal and an amplifier with a 16V power supply.

The data obtained are images taken with a Basler camera using illumination from a LED and a 10 μs shutter time. From Kremer *et al.*[1] it became clear that the damping of the resonant oscillation takes around 50 ms. Even though the camera has a 10 μs shutter time, the time to take one image and process it takes around 10 ms. So the damping happens too fast for the camera to take enough images to record the damping of one excitation. Stroboscopic imaging with the shutter is then used. The excitation is repeated, in the assumption that the excitation is reproducible. The images are taken with an increasing time of 1 ms between two consecutive images to eventually record the whole damped oscillation.

3.1.2 Synchronized triggering

In order to take the images at the right time after the field is turned back on, with an increase in time every image, both the signal generator and the camera are externally triggered with two signals from an Arduino Mega. The burst function of the signal generator is used. Here, when externally triggered, it burst out 23900 cycles every 0.6 s so that the field is turned off for 100 cycles, which corresponds with 2.5ms for a 40 kHz signal.

The increasing time after each image is obtained by also externally triggering the camera, but with a slightly different frequency, such that the falling slope of the signal increases 1 ms every period with respect to the trigger signal of the signal generator. For a clear visualization of the signals and the programming of the Arduino see figure 3.

[4]The building of the acoustic levitator is roughly based on the explanation from: http://www.instructables.com/id/Acoustic-Levitator/. Only here a signal generator is used for the 40 kHz signal instead of an Arduino.

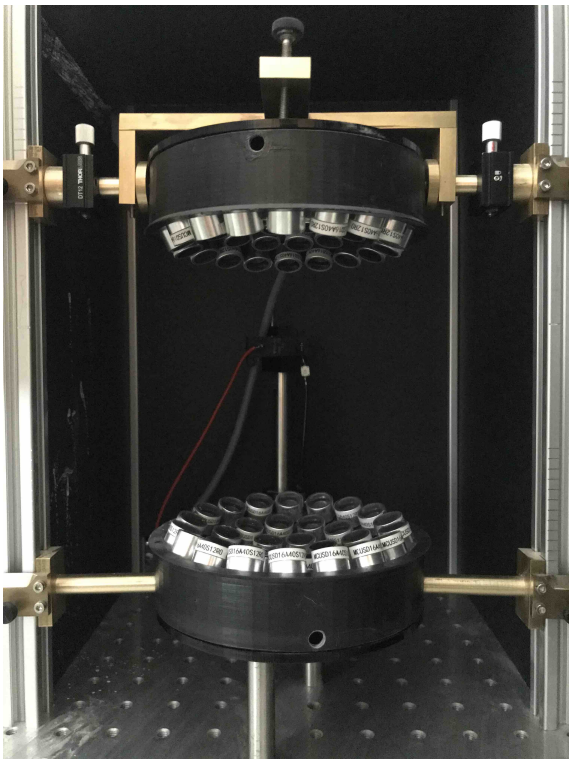

Figure 1: This is the acoustic levitator consisting of two panels filled with transducers that have a sharp resonance at 40 kHz. Also the LED for illumination of the droplet is shown and the cardboard surrounding the levitator to minimalize air fluctuations.

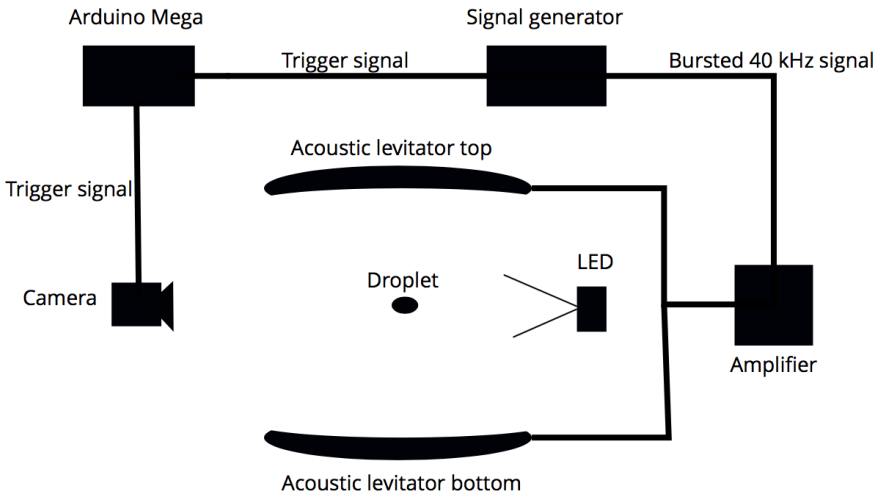

Figure 2: This is a schematic overview of the setup with the two triggering signals from the Arduino to the camera and the signal generator, the acoustic levitator, driven by the amplified bursted signal and the sample, illuminated by a LED.

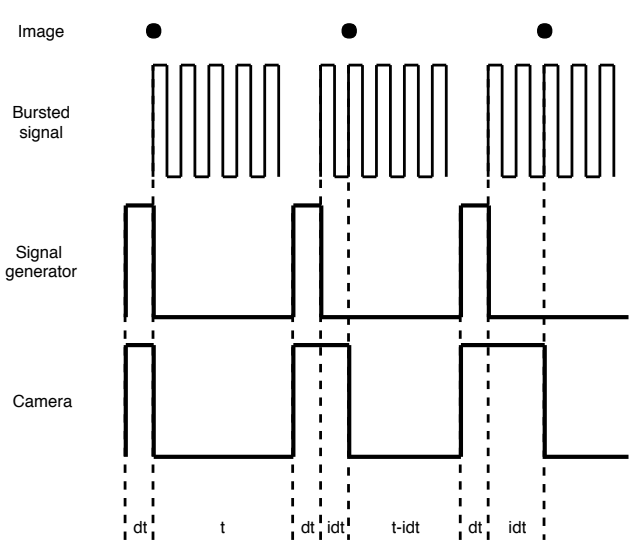

(a)

```
while (1==1) {
  if (state == 0) {
    if (t - i*dt < 0) {
      i = 0;
      }
    digitalWrite(PIN, HIGH);
    digitalWrite(PINSIG, HIGH);
    delay(dt);
    digitalWrite(PINSIG, LOW);
    delay(i*dt);
    state = 1;
  }
  else {
    digitalWrite{PIN, LOW};
    delay(t - i*dt);
    state = 0;
    i = i+1;
  }
  }
```

(b)

Figure 3: (a) Here the two signals are shown for triggering the signal generator and the camera. At the top of the figure it is shown that on the falling edge the signal generator is triggered and a signal is bursted to the acoustic levitator. The dots represent when the images are made. (b) This is the code used to program the two signals of the Arduino with a frequency difference in the falling edge of the signal due to the iteration over i. PIN is the signal for the camera and PINSIG for the signal generator. The else loop is made to ensure a continuous signal.

3.1.3 Limitation of distortions

The airflow around the acoustic levitator can result in translational vibrations of the droplet, and since this translation pushes the droplet towards high pressure regimes other oscillations can also be developed. To minimize this airflow the setup should be sealed from the outside air. Here the levitator is surrounded with cardboard, conveniently also blocking light coming in from the outside.

The size of the droplet is also of much influence. According to Theory it is shown that the droplet should not be too small, order of nm. However, from the experiment it becomes clear that a droplet should also not be too big. Droplets with a larger radius than 1.5 mm can drop too much into a high pressure regime when the field is turned off, simply because a larger radius reaches further down when falling the same distance as a smaller droplet. Because of this the bottom of the droplet gets a push back up with a greater upward force at the bottom than around the edges. This results in deformation of the droplet, in a way inconsistent with the elliptical shape from the resonant oscillation. Another effect that a too big droplet has is that some higher mode surface oscillation can occur. Images of these unwanted deformations are shown in figure 4. The experimental data also suggests that this plays a bigger role for droplets of water than for droplets of a colloidal suspension, since these deformations have not been observed in the measurements of the colloidal suspension.

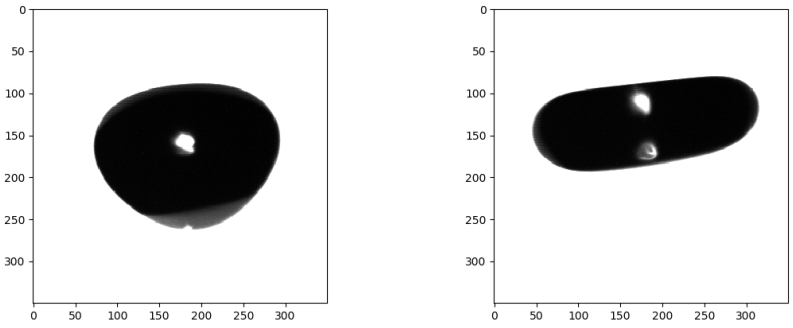

(a) (b)

Figure 4: Here the resulting unwanted deformation of a water droplet is shown. This deformation arises because the droplet has a too big volume equal sphere radius, greater than 1.5 mm. (a) The asymmetrical shape of the droplet suggests the presence of higher modes of oscillation. (b) The concave bottom is the result of the droplet dropping too far in a high pressure regime when the field is turned off and is then pushed back with greater force when the field is turned back on.

3.2 Data analysis

The raw data obtained from this setup are images of the droplet, elliptically shaped due to their oscillation and the pressure forces of the acoustic field, as is shown in figure 5(a). From this image the radius of the ellipse needs to be calculated to eventually determine the damping of the resonant oscillation obtained from excitation of the droplet. From here the viscosity can be calculated via equation (8) from Theory, section 2.2.

3.2.1 Radius determination

The radius determination is done using Python with a script that first selects all the pixels on the edge of the droplet in order to fit an ellipse to that edge. The edge detection is done using the difference in intensity between the gray-scaled pixels of the droplet and the background. Because of the illumination from the LED the background is so bright it reaches the maximum pixel intensity, whereas the droplet does not.

The fitting of the ellipse is done with the use of a class of functions created by Ben Hammel and Nick Sullivan-Molina.[7] In this class the ellipse is fitted to data points of high intensity, so in order to have the right data as input the image is inverted. Now the background becomes dark with low intensity pixels and only an elliptical edge of high intensity is left. The inverted image and the edge of the droplet are shown in figure 5(b) and 5(c).

Now an ellipse is fitted to the edge, taking the angle of the droplet into account since the droplet sometimes can get tilted by a few degrees, as is shown in figure 5(d). From the fit parameters the horizontal radius is calculated using equation(11), as described in Theory, section 2.3. In Appendix B.1 an overview of the calculation using Python is given. From here the radius as a function of time is created in order to determine the damping of the oscillation, as is shown in figure 6.

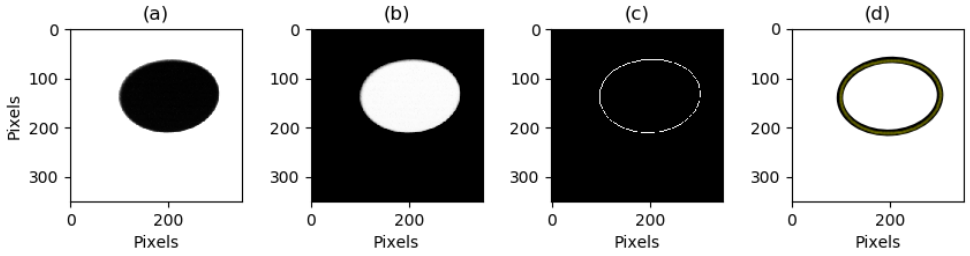

Figure 5: (a) An image of the raw data. (b) The image with inverted pixel intensities. (c) The detected edge of the droplet with high intensity. (d) The fitted ellipse to the edge of the droplet.

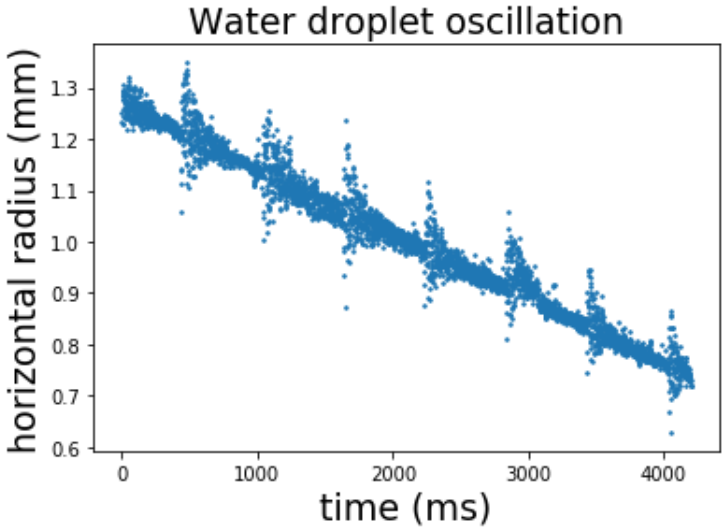

Figure 6: Here the horizontal radius of the water droplet is plotted as a function of time. There are 6 full periods of damping after excitation, clearly visible by the increase and decrease of the spread in radii. The slope of the plot is negative because the droplet shrinks during the measurement due to evaporation.

3.2.2 Pixel size determination

As one can see from figure 5 the image is given in number of pixels. This is not a problem for the determination of the damping constant, but since the volume equal sphere radius is needed for the calculation of the viscosity a pixel size determination is needed. This is done by taking an image of the millimeter stripes of a ruler, with an intensity difference with respect to the rest of the ruler. This difference can be made bigger by increasing the shutter time of the camera. Using this image the number of pixels between two millimeter stripes is calculated line by line and averaged over 289 measurements. The pixel size determined by this method is: 15.57 ± 0.28 μm per pixel, with the uncertainty calculated from the standard deviation of the 289 measurements.

3.2.3 Damping fitting

From the radius as function of time, shown in figure 6 (a) a second oscillation is visible, especially in the tail of the envelope. This could be due to higher oscillation modes present. Because of this two different analysis are used. For the first analyses it is used that the decay of the amplitude is clearly visible. Equation(13) is then used to calculate the damping since it relies on the standard deviation of the radius. For the second analysis the oscillation in the radius is used directly and the damping is calculated from equation (12).

Because the measurement takes long enough for the droplet to evaporate a significant portion of its volume a downward slope of the radius is visible. To eliminate this effect for the fist method equation (13) will be divided by the equilibrium radius r_0 and for the second method a linear evaporation term will be added to equation (12), giving the following result:

$$\frac{\sigma_r}{r_0} = \frac{1}{\sqrt{2}r_0} A e^{\frac{-t}{\tau}}, \tag{14}$$

$$r(t) = r_0 + A e^{-\frac{t}{\tau}} cos(2\pi f t) + \xi - kt. \tag{15}$$

In order to fit the data shown in figure 6 to these equations it needs to be separated in periods. This is done using Python and shown in figure 7(a). For the fitting to equation (14) the standard deviation is calculated for bins of 100 measurements, moving the bin by one point each calculation. The bin size is chosen so it contains at least 2 periods of the second oscillation which is enough to average over. An example of the fitting to the standard deviation and to the data directly are shown in figure 7(b) and 7(c). In Appendix B.2 an overview of the fitting in Python is given.

The uncertainties of τ are calculated taking the square root of the covariance of the fit parameters provided by the scipy.optimize package from Python. Then for the viscosity the uncertainties follow from calculation with the minimal and maximum value of τ.

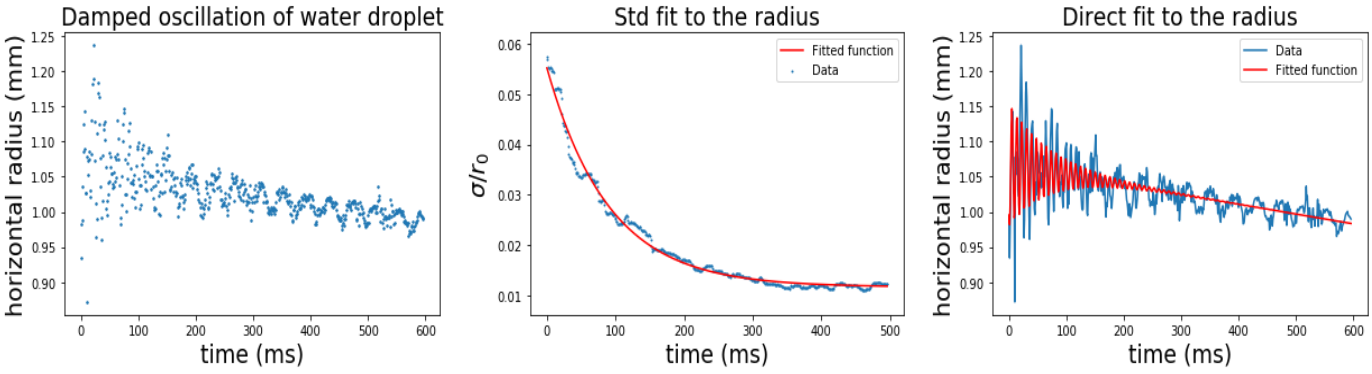

(a) (b) (c)

Figure 7: (a) The horizontal radius of one period of the damping after excitation is shown. (b) The standard deviation of that radius, divided by the equilibrium radius for bins of 100 measurements is shown. The continuous line is a fit to the data following the model described by equation (14). (c) Equation (15) is directly fitted to the data. The data is presented as connected lines to check the frequency of the fitted function.

4 Results

The remote viscosity measurement is done for two different droplets, a water and a colloidal droplet. The results for these droplets will be presented separately. For each droplet the time between images increases with 1 ms. Here the data is presented as if there is 1 ms between consecutive images instead of the 601 ms that is actually between them, because the droplet is excited every measurement. Also the time on the x-axis is set to 0 for each period. This is done so a time indication of the damping becomes visible, but note that in this way the evaporation looks misleadingly fast.

For the fitting of the damping of the resonant oscillation a cutout is made of every period of damping. This cutout consists out of 597 measurements. There are 600 images in one period, but the last three images are left out since they are made during the excitation of the next period. Also the vertical radius is used for the fitting since it changes less and is smaller due to its elliptical shape, which resulted in data with less distortions.

4.1 Water

First a water droplet is levitated. Here 4200 images are made and with an excitation every 0.6 s the total measurement takes 42 minutes. Because of this the droplet evaporates during the measurement. The vertical radius as a function of time is shown in figure 8. In this figure a downward slope is visible which means a decreasing average radius, which is due to the evaporation of the droplet.

In the measurement 6 damped periods of oscillations are visible. Each period and both analysis methods, as discussed in section 3.2.3 are shown in figure 9. For each period the average vertical and horizontal radius is calculated. From here the average volume V and volume equal sphere radius a are calculated such that a calculation can be made of the viscosity μ using equation (8). The results of this are given in table 1, where the subscripts 1 and 2 represent the fitting to the standard deviation and directly to the data respectively.

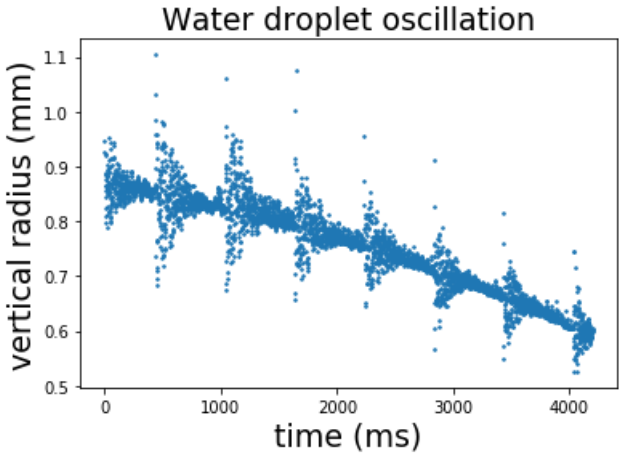

Figure 8: Here the vertical radius of the water droplet is shown as a function of time. 4200 Measurements are made during 42 minutes imaging 6 full periods of damped oscillations. The downward slope is due to evaporation of the water droplet.

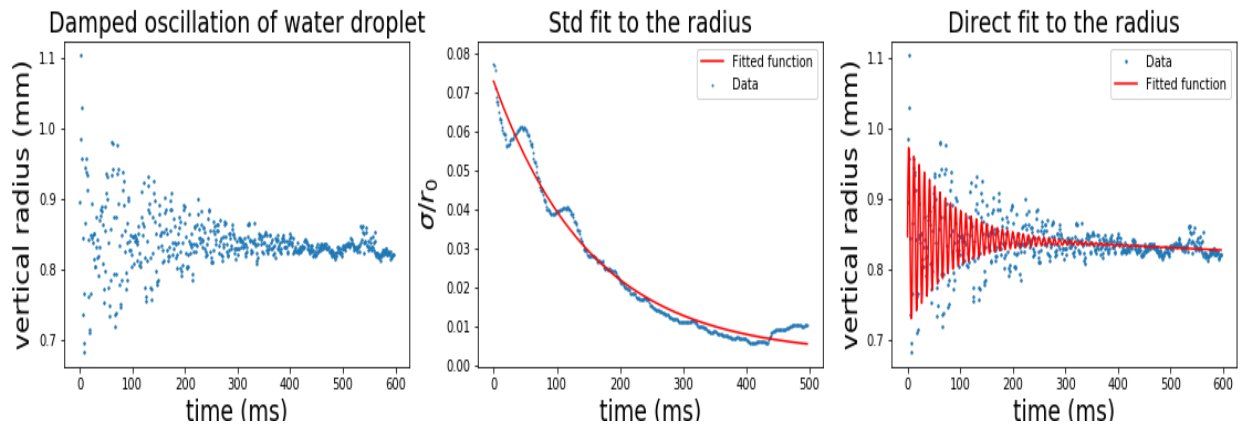

(a)

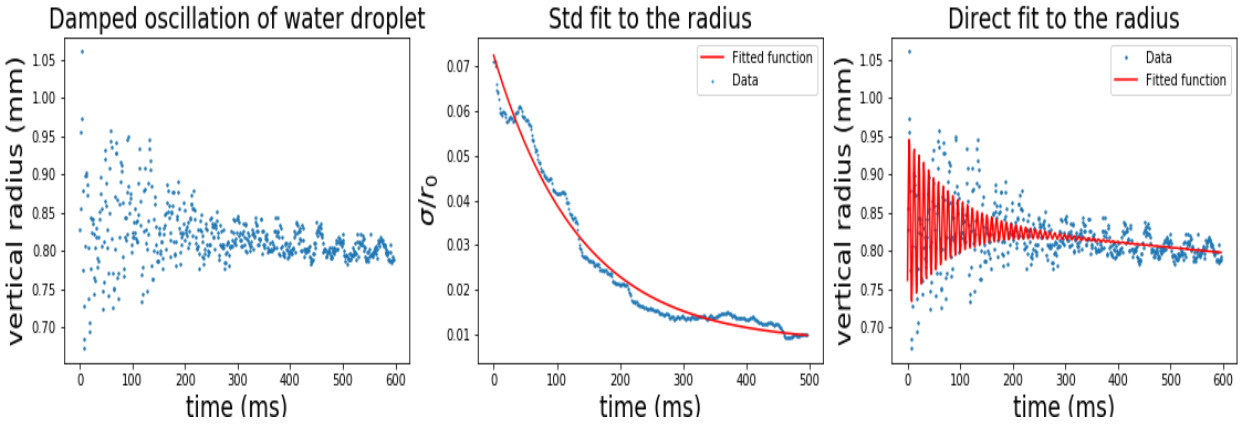

(b)

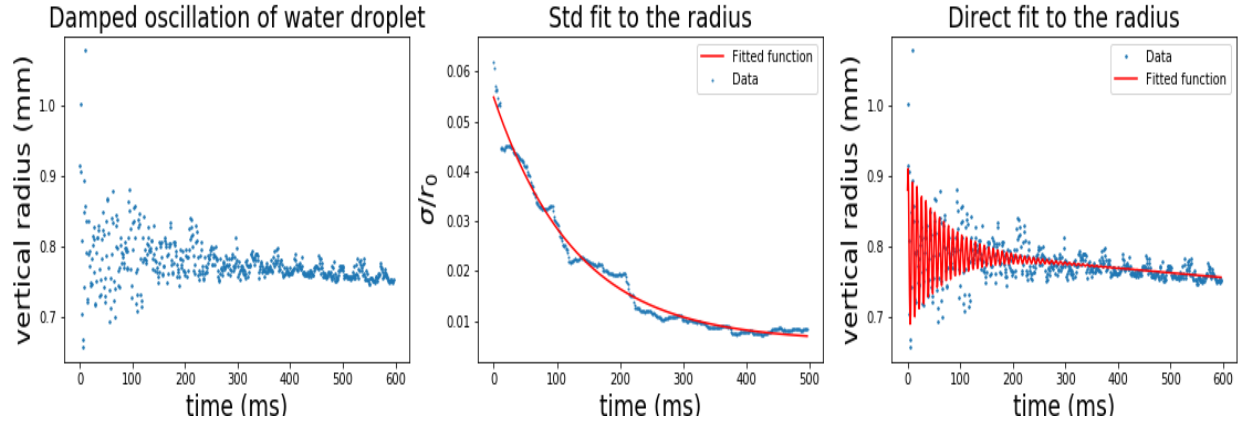

(c)

Figure 9: The radius measurement of the water droplet is cut out per period. Period 1 to 6 are represented by figures (a) to (f). Left: the vertical radius as function of time for the water droplet is shown. Middle: the the standard deviation divided by average radius σ/r_0 is fitted to equation (14). Right: the data is directly fitted to equation (15).

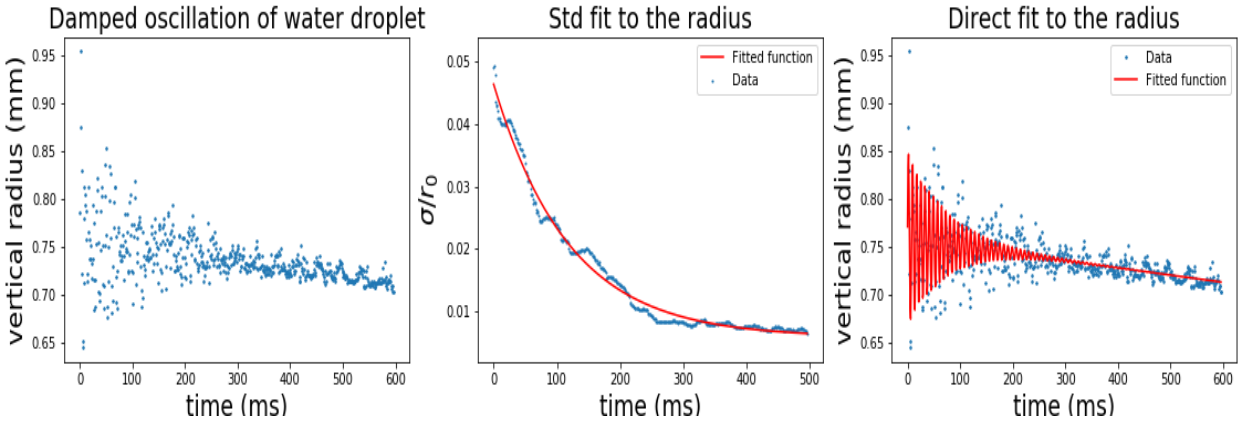

(d)

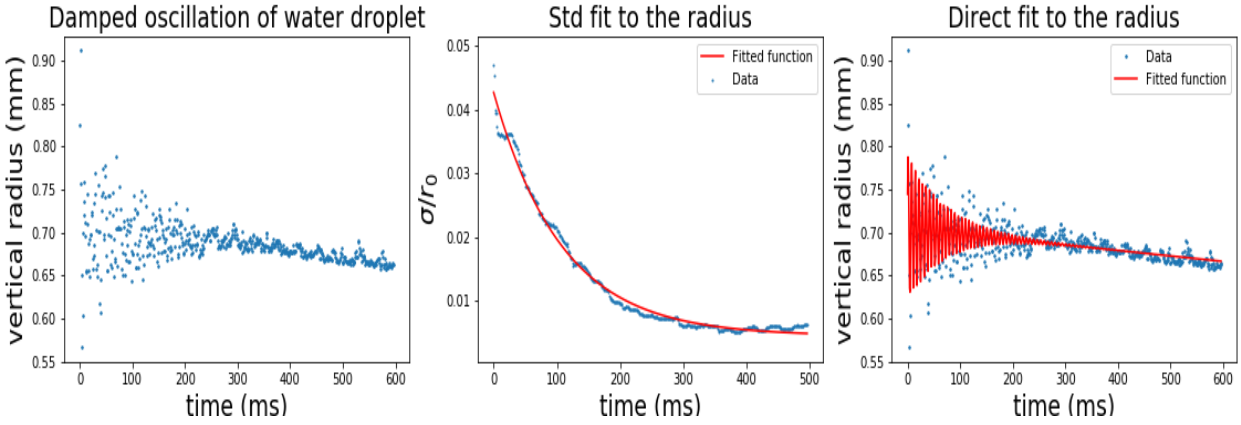

(e)

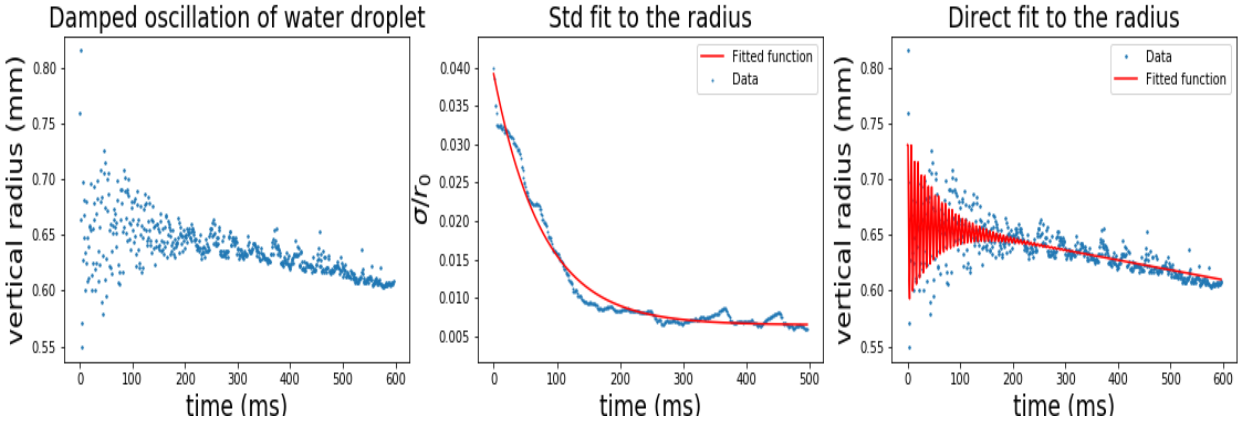

(f)

Figure 9: Continued.

Table of experimental data of water droplet per period of damping						
Period	τ_1 (ms)	τ_2 $(ms)^*$	V (mm^3)	a (mm)	$\mu_1(mPa \cdot s)$	μ_2 $(mPa \cdot s)^*$
1	155.1 ± 3.1	83 ± 273	4.91	1.05	1.42 ± 0.03	2.65 ± 0.89
2	136.0 ± 2.8	83 ± 318	4.71	1.00	1.47 ± 0.03	2.40 ± 0.67
3	130.2 ± 1.9	72 ± 290	3.45	0.94	1.35 ± 0.02	2.45 ± 0.65
4	118.9 ± 1.6	76 ± 379	2.80	0.87	1.27 ± 0.02	1.99 ± 0.41
5	108.3 ± 1.2	72 ± 397	2.27	0.82	1.24 ± 0.01	1.76 ± 0.35
6	77.8 ± 1.2	56 ± 383	1.73	0.74	1.40 ± 0.02	1.45 ± 0.29

Table 1: Here the results are represented, calculated from the radius measurements of a water droplet. For each period of damping two different analysis are used. τ_1 and μ_1 are derived from analyzing the decay of the standard deviation of the radius. τ_2 and μ_2 are derived from analyzing the data directly. From the radii the average volume V and average volume equal sphere radius a are calculated to eventually derive the viscosity according to equation (8).
$*$ The uncertainty is unphysically large for τ_2, such that this data must be discarded.

4.2 Colloidal droplet

Next the viscosity is measured of a levitated water droplet suspended with 1 μm particles based on polymethacrylate. The mass concentration of the colloids at the start of the measurement is 10%. The colloids with a density of 1.19 $g \cdot cm^{-3}$[8] are suspended in water with a density of 0.997 $g \cdot cm^{-3}$. In total 7200 images are taken, which takes 72 minutes in total. This is enough time for the water in the droplet to fully evaporate such that a solid disc shape remains, containing the colloidal particles. During this evaporation the density increases, and is calculated from the initial mass concentration and the evaporation rate of water in the droplet. The horizontal and vertical radii are both plotted as function of time in figure 10.

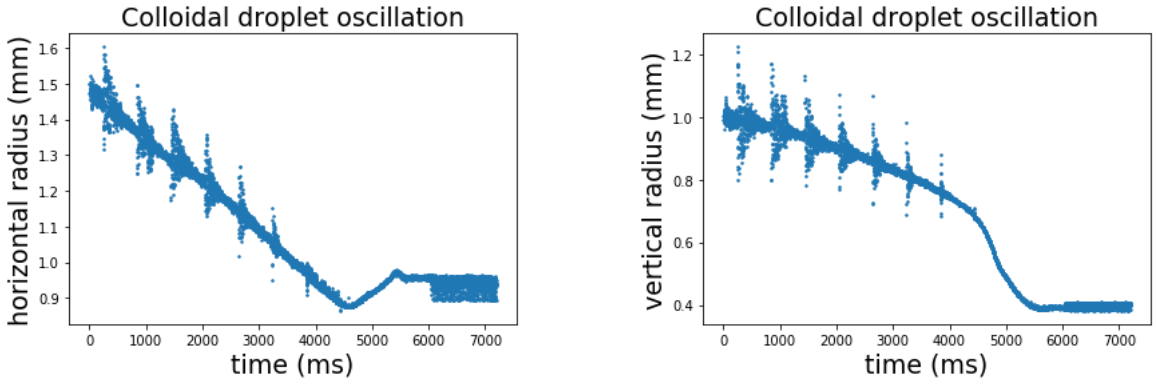

(a) (b)

Figure 10: (a) Is the horizontal radius of the colloidal droplet and (b) is the vertical radius. The measurement consists of 7200 images and takes 72 minutes. The downward slope is due to evaporation of the colloid suspension. When the droplet is evaporated enough the excitation is not longer visible in the radius and the droplet loses its ellipsoidal shape.

The measurement of the horizontal radius can be divided into two regions. One with the negative slope where the droplet is evaporating but still liquid and the other from the positive slope where the droplet is deforming, becoming flatter and eventually becoming fully solid. For the viscosity measurement of this colloidal droplet the first region is of interest since this is the only place where the excitation is visible in the radius of the droplet. For the second region the droplet loses its ellipsoidal shape so the analysis of the elliptical edge is no longer sufficient here. The cutouts from the data, done the same way as for the water droplet and both fitting results of the damping to the standard deviation divided by the average radius and to the data directly are shown in figure 11. The results from fitting the damping τ, calculating the volume equal sphere radius a, the changing density and the viscosity are represented in table 2. Once again the subscripts 1 and 2 represent the fitting to the standard deviation and directly to the data respectively.

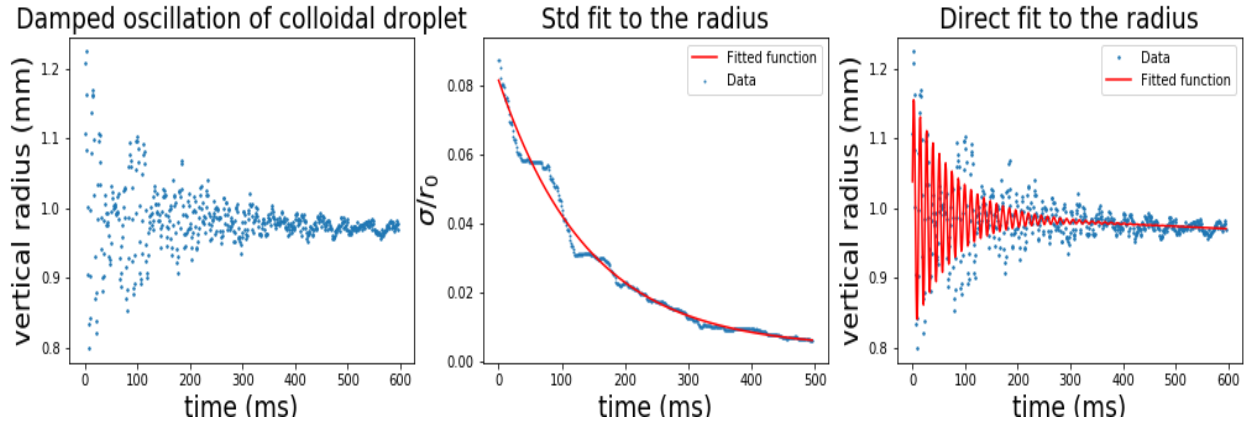

(a)

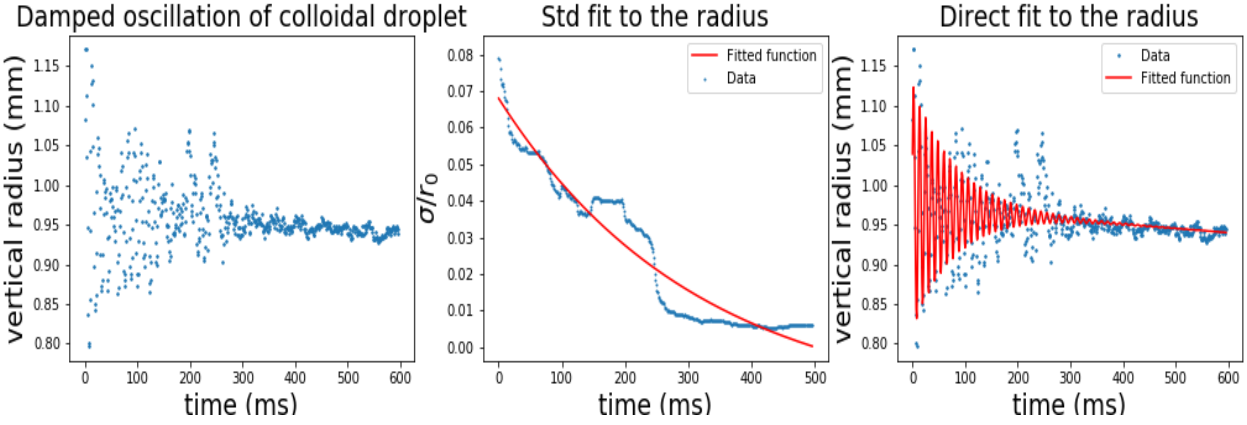

(b)

Figure 11: The radius measurement of the colloidal droplet is cut out per period. Period 1 to 6 are represented by figures (a) to (f). Left: the vertical radius as function of time for the colloidal droplet is shown. Middle: the standard deviation divided by average radius σ/r_0 is fitted to equation (14). Right: the data is directly fitted to equation (15).

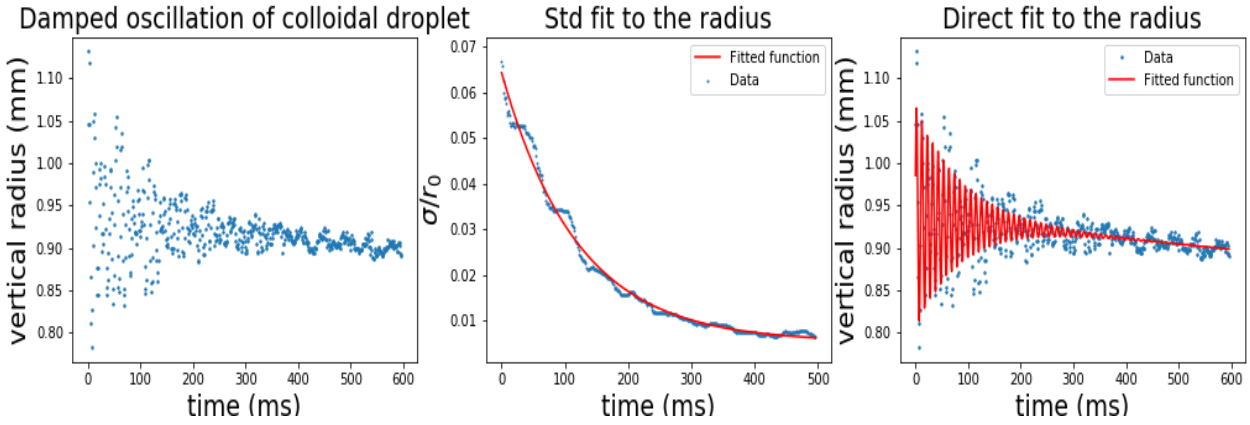

(c)

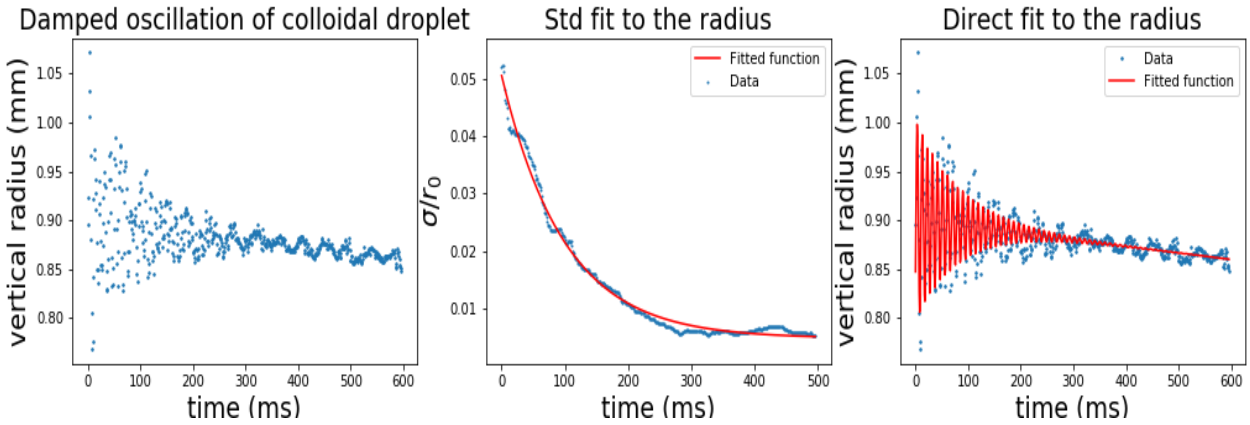

(d)

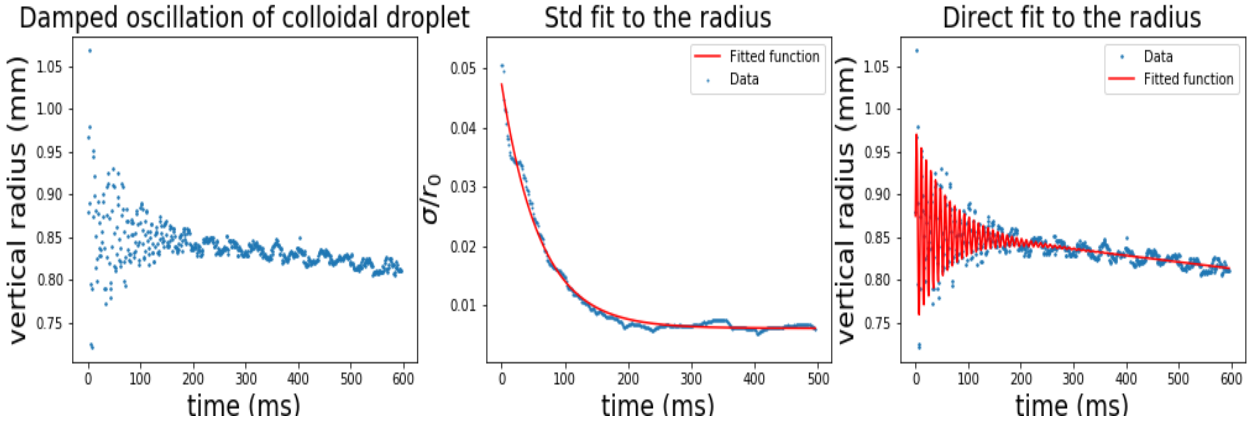

(e)

Figure 11: Continued.

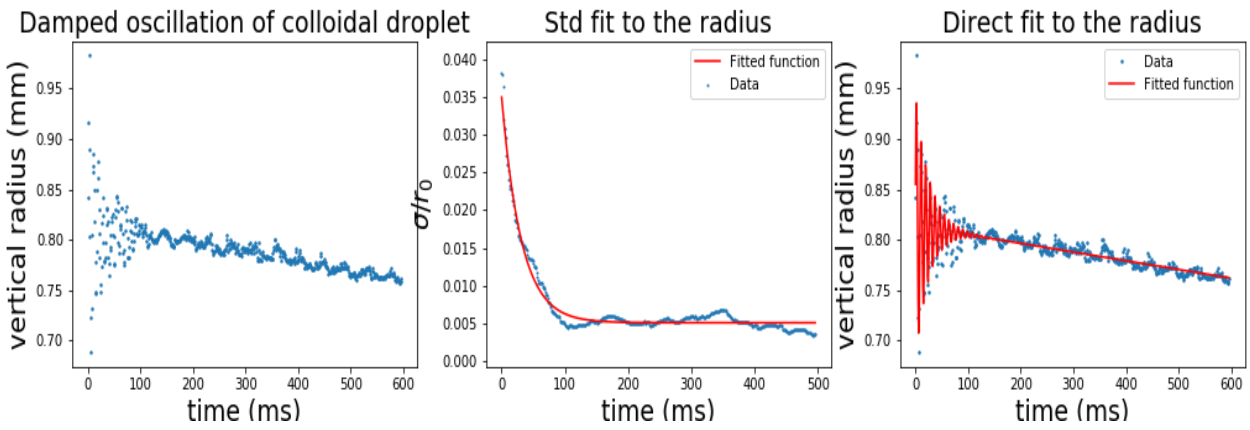

(f)

Figure 11: Continued.

Table of average experimental data per period of damping							
Period	τ_1 (ms)	τ_2 $(ms)^*$	V (mm^3)	a (mm)	ρ $(g \cdot cm^{-3})$	μ_1 $(mPa \cdot s)$	μ_2 $(mPa \cdot s)^*$
1	142.6 ± 2.1	75 ± 198	4.63	1.25	0.9989	2.19 ± 0.03	4.16 ± 1.8
2	314.0 ± 20	82 ± 232	3.99	1.19	0.9992	0.90 ± 0.06	3.45 ± 1.4
3	119.9 ± 1.4	87 ± 281	3.48	1.14	0.9995	2.17 ± 0.03	2.99 ± 1.0
4	99.4 ± 1.1	85 ± 361	2.94	1.08	1.000	2.35 ± 0.03	2.74 ± 0.7
5	60.9 ± 0.64	62 ± 274	2.41	1.01	1,001	3.35 ± 0.04	3.29 ± 0.8
6	31.0 ± 0.50	26 ± 158	1.92	0.93	1.002	5.58 ± 0.09	6.66 ± 1.1

Table 2: Here the results are represented, calculated from the radius measurements of the colloidal droplet with 1 μm particles based on polymethacrylate. For each period of damping the constant τ is derived in two different ways. τ_1 and μ_1 are derived from analyzing the decay of the standard deviation of the radius. τ_2 and μ_2 are derived from analyzing the data directly. From the radii the average volume V, average volume equal sphere radius a and density ρ are calculated to eventually derive the viscosity according to equation (8).
$*$ The uncertainty is unphysically large for τ_2, such that this data must be discarded.

From the data in figure 11 (b) it can be seen that the fit for τ_1 is not representable for the data. Due to some distortions in the data a too high value for the damping constant is calculated from the fit resulting in a too low viscosity. Also the second method of fitting results in such high uncertainties, roughly 4 times the estimated value, that it will not be used to evaluate the change in viscosity due to evaporation. In the discussion, section 5, a broader explanation for these choices will be provided. The change in viscosity due to evaporation for the colloidal droplet calculated from the first fitting method discarding the second period is shown in figure 12.

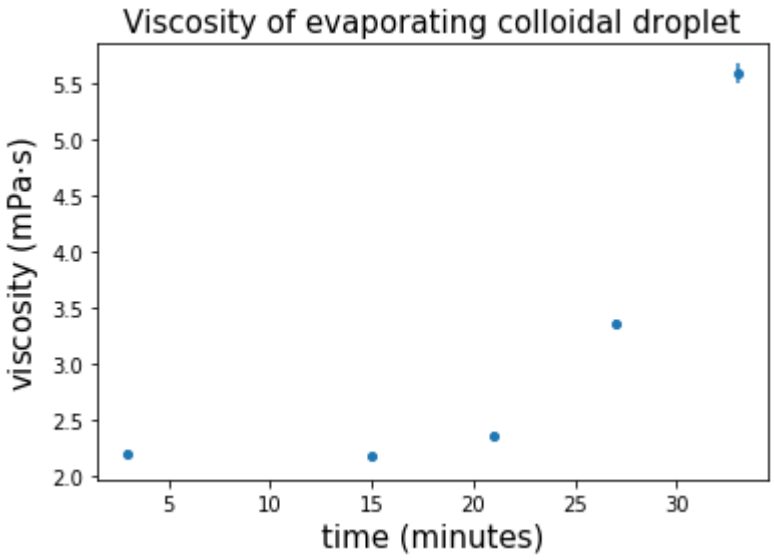

Figure 12: Here the time evolution of the viscosity is shown for the colloidal droplet. The viscosity is obtained using the first fitting method discarding the value for the second period. On the x-axis the time is given in minutes. Here in contrast to the other presentations of the data the 0.6 s between two excitations is included since here the timescale for evaporation is important instead of the damping constant.

In region 2 the droplet loses its ellipsoidal shape and decreases in size rapidly in comparison with region 1. The horizontal radius increases, flattening out the droplet, and the surface becomes more edgy. The acquired radii are no longer representative for the droplet since an ellipse is fitted to a no longer elliptical shape. See figure 13 for 9 images of the droplet in region 2 of the measurement. Here the images show 14 minutes of evaporation 47 minutes after the start of the measurements. The first 8 images with 2 minutes between them show the deformation of the droplet and a cumulation at the border resulting in a more edgy surface. The last two images are two consecutive images from the solid residue of the evaporated colloidal suspension. In this last step a dent appears and the residue starts rotating.

This last step seems to be consistent with the findings of Agthe *et al.*, where they found "a two-step process where the particles cluster into an intermediate disordered precursor that rapidly transforms into large, well ordered mesocrystals".[9] They are left with a dry hollow capsule which can be compared with the dent and is also observed in repetition of the experiment. Figure 14 is an image of the evaporated colloidal droplet of this experiment showing the dent and hollow capsule shape. Transition electron microscopy is needed to give a more elaborate observation of the crystallization of the residue.

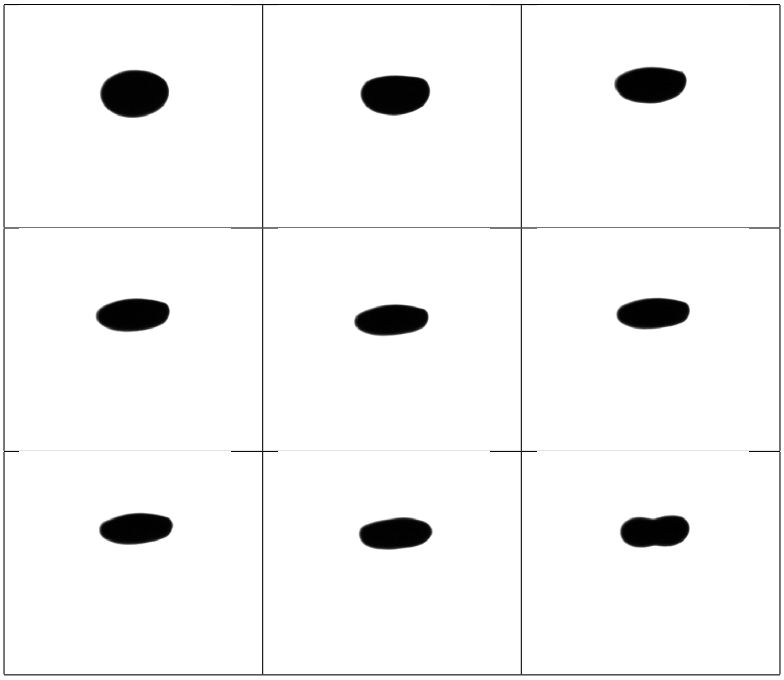

Figure 13: Here 9 images of the droplets crystallization progress are shown, covering in total 14 minutes of the experiment. The first image (top left) is taken 47 minutes after the start of the measurement and the last image (bottom right) 61 minutes. There are 2 minutes between all the first 8 images. The last two images are consecutive images showing the rotation and the dent of the solid, which is not spherical symmetric.

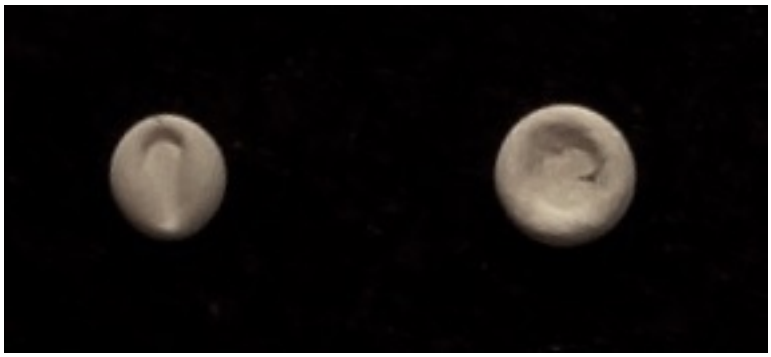

Figure 14: These are the residues of the evaporated colloidal droplet with 1 μm particles based on polymethacrylate. Left is the residue with the dent for which the evaporation is analyzed. The one on the right is the residue from a repetition of the experiment also showing the hollow capsule shape as Agthe *et al.*[9] described.

5 Discussion

As briefly mentioned in 4.2 of the results the second analysis method where the damping is fitted directly to the data result in unacceptable large uncertainties, varying from 2.6 to 6.1 times the estimated value of τ_2. By eye it is visible from figure 11 that the fit estimates a too low value for τ_2. The high uncertainties can also follow from an extra oscillation becoming clear in the most damped region of the envelope of the data which is averaged out in the first analysis method where the fit is made to the standard deviation. In order for the second method to work, improvements must be made to the stability of the trap and the excitation method.

Also in the results the measurement of the second period of the colloidal droplet is discarded. This is done because the fit to the standard deviation gave an uncertainty at least 10 times higher than the other uncertainties. This distortion is also visible in the radius measurement, giving a higher standard deviation and a wrong fit for τ_1 resulting in a higher value than expected. The choice to discard this data is legitimate because these distortions are observed before, for instance when someone walked by the levitator.

For increasing the reliability of the measurements faster imaging of the radius of the droplet is needed. A high speed camera, for instance, can measure the damping of the resonant oscillation in one excitation. This has the benefits that the assumption that the excitation is reproducible is no longer needed. Also evaporation does not play a role during one excitation so averaging the volume and with that the volume equal sphere radius per period of excitation is no longer needed. Another improvement could be made regarding the air flow in the setup. The measurement can be distorted much by airflow and especially hot or cold air, fluctuating the temperature in the setup, since viscosity is highly temperature dependent. An air sealed box around the setup will eliminate more of these distortions than the cardboard that is used now.

The acoustic levitator can be used for remote measurements of viscosity and surface tension, but another region of interest that could be explored further is, as Seddon *et al.*[10] suggested, the dynamics in a droplet since there is no friction with a wall since the whole droplet has an uniform air-liquid interface. Also the crystallization of the colloidal droplet inside the acoustic levitator is interesting for further research.

6 Conclusions

We investigated the viscosity of acoustically levitated droplets. The free decay method is used where the field is turned off for 2.5 ms. With stroboscopic imaging the damping of the resonant oscillation is imaged. The camera is triggered ever 601 ms and the excitation every 600 ms resulting in effectively imaging the damping every 1 ms. The calculation of the radius of the droplet is done by fitting an ellipse to the edge. From the measured radius the damping constant τ is calculated using two different analyses, a fit to the standard deviation of the radius, giving τ_1, μ_1 and a fit to the radius directly, giving τ_2, μ_2. Here the second method was found to be insufficient for the obtained data due to too many distortions in the damped oscillation, resulting in a too short fit for τ_2 with uncertainties roughly 4 times as big as the initial value.

Measurements are done with a water and a colloidal droplet with 1 μm particles based on polymethacrylate. For the water droplet in 6 periods of measurements an average viscosity of: $\mu_1 = 1.36 \pm 0.02\ mPa \cdot s$ was found. Which is off by a factor 1.36 from the literature value of $\mu = 1.002\ mPa \cdot s$. And for the colloid an increasing viscosity due to evaporation from $\mu_1 = 2.19 \pm 0.03\ mPa \cdot s$ to $\mu_1 = 5.58 \pm 0.09\ mPa \cdot s$ was measured.

7 References

References

[1] J. Kremer, A. Kilzer, and M. Petermann, Review of Scientific Instruments **89**, 015109 (2018).

[2] H. Lamb, *Hydrodynamics*, 6th ed., Cambridge University Press, Cambridge, (1932).

[3] H.D. Young and R.A. Freeman, *Sears and Zemansky's University Physics with Modern Physics Technology update*, Pearson, 13th ed. (2014).

[4] D. Langstaff, M.Gunn, G.N. Greaves, A. Marsing and F. Kargl, Review of Scientific Instruments **84**, 124901 (2013).

[5] E. Becker, W.J. Hiller, and T.A. Kowalewski, Journal of Fluid Mechanics, **231**, 189 (1991).

[6] A. Prosperetti, Journal of Fluid Mechanics, **100**(2), 333 (1980).

[7] B. Hammel, N. Sullivan-Molinaleast, *least-squeres-ellipse-fitting*, Python code from: https://github.com/bdhammel/least-squares-ellipse-fitting/blob/master/ellipses.py, 2-5-2018.

[8] Sigma-Aldich, Certificate of Analysis, from: https://www.sigmaaldrich.com/catalog/CertOfAnalysisPage.do?symbol=90875&LotNo=BCBT9216&brandTest=SIAL&returnUrl=%2Fproduct%FSIAL%2F90875, 31-5-18.

[9] Michael Agthe, Toms S. Plivelic, Ana Labrador, Lennart Bergstrm, and German Salazar-Alvarez, Nano Letters, 2016 **16** (11), 6838-6843.

[10] A.M. Seddon, S.J. Richardson, K. Rastogi, T.S. Plivelic, A.M. Squires and C. Pfrang, Journal of Physical Chemistry Letters, 2016, **7** (7), pp 13411345.

A Appendix

A.1 Appendix

Here the derivation of equation (5) for the average dissipation F_{av} will be calculated starting with the equations (2), (3) and (4) respectively:

$$\begin{aligned}
2F &= \mu \iint \frac{\partial q^2}{\partial r} r^2 d\omega = \mu r^2 \frac{\partial}{\partial r} \iint q^2 d\omega, \\
r^2 \iint q^2 d\omega &= \frac{\partial}{\partial r} \iint \phi \frac{\partial \phi}{\partial r} r^2 d\omega, \\
\phi &= A \frac{r^n}{a^n} S_n \cos(\sigma t + \epsilon).
\end{aligned}$$

From the combination of equations (3) and (4) it follows that:

$$\begin{aligned}
\iint \phi \frac{\partial \phi}{\partial r} r^2 d\omega &= \iint \frac{r^n}{a^n} \frac{n r^{n-1}}{a^n} S_n^2 d\omega A^2 \cos^2(\sigma t + \epsilon) r^2, \\
\iint \phi \frac{\partial \phi}{\partial r} r^2 d\omega &= r^2 n \Big(\frac{r}{a}\Big)^n \Big(\frac{r^{n-1}}{a^n}\Big) \iint S_n^2 d\omega A^2 \cos^2(\sigma t + \epsilon), \\
\iint \phi \frac{\partial \phi}{\partial r} r^2 d\omega &= n a \Big(\frac{r}{a}\Big)^{2n+1} \iint S_n^2 d\omega A^2 \cos^2(\sigma t + \epsilon).
\end{aligned}$$

Combining this result with equations (3) gives:

$$\begin{aligned}
r^2 \iint q^2 d\omega &= \frac{\partial}{\partial r} n a \Big(\frac{r}{a}\Big)^{2n+1} \iint S_n^2 d\omega A^2 \cos^2(\sigma t + \epsilon), \\
r^2 \iint q^2 d\omega &= \frac{n a (2n+1)}{a} \Big(\frac{r}{a}\Big)^{2n} \iint S_n^2 d\omega A^2 \cos^2(\sigma t + \epsilon), \\
r^2 \iint q^2 d\omega &= n(2n+1) \frac{r^2}{a^2} \Big(\frac{r}{a}\Big)^{2n-2} \iint S_n^2 d\omega A^2 \cos^2(\sigma t + \epsilon), \\
\iint q^2 d\omega &= \frac{n(2n+1)}{a^2} \Big(\frac{r}{a}\Big)^{2n-2} \iint S_n^2 d\omega A^2 \cos^2(\sigma t + \epsilon).
\end{aligned}$$

Now using the above result combined with equation (2) gives the expression for the dissipation F in the approximation that a=r:

$$\begin{aligned}
2F &= \mu r^2 \frac{\partial}{\partial r} \iint q^2 d\omega, \\
2F &= \mu r^2 \frac{\partial}{\partial r} \frac{n(2n+1)}{a^2} \Big(\frac{r}{a}\Big)^{2n-2} \iint S_n^2 d\omega A^2 \cos^2(\sigma t + \epsilon), \\
2F &= \mu r^2 \frac{n(2n+1)(2n-2)}{a^3} \Big(\frac{r}{a}\Big)^{2n-3} \iint S_n^2 d\omega A^2 \cos^2(\sigma t + \epsilon), \\
2F &= 2n(2n+1)(n-1) \frac{\mu}{a} \iint S_n^2 d\omega A^2 \cos^2(\sigma t + \epsilon).
\end{aligned}$$

Finally taking the average value of the cosine squared gives the wanted expression for the average dissipation F_{av}:

$$2F_{av} = n(2n+1)(n-1)\frac{\mu}{a}\iint S_n^2 d\omega A^2.$$

A.2 Appendix

Here the derivation of equation (8) for the dynamic viscosity μ will be calculated starting with the equation (1) for energy and dissipation and filling in the equations (5) and (7):

$$\begin{aligned}
&\frac{d}{dt}(T+V) = -2F_{av},\\
&\frac{d}{dt}\frac{1}{2}\rho n a \iint S_n^2 d\omega A^2 = -n(n-1)(2n+1)\frac{mu}{a}\iint S_n^2 d\omega A^2,\\
&\frac{d}{dt}\frac{1}{2}A^2 = -(n-1)(2n+1)\frac{\mu}{\rho}\frac{1}{a^2}A^2,\\
&\frac{dA}{dt} = -(n-1)(2n+1)\frac{\mu}{\rho a^2}A.
\end{aligned}$$

This leads to a differential equation. We know that A relates to $e^{-t/\tau}$ so the damping constant τ is given by:

$$\tau = \frac{1}{(n-1)(2n+1)}\frac{\rho a^2}{\mu}.$$

The dynamic viscosity μ can than be calculated via the following formula:

$$\mu = \frac{\rho a^2}{\tau(n-1)(2n+1)}.$$

B Appendix

B.1 Appendix

```
#eigenvectors are the coefficients of an ellipse in general form
#a*x^2 + 2*b*x*y + c*y^2 + 2*d*x + 2*f*y + g = 0 [eqn. 15) from (**)
or (***)
a = self.coef[0,0]
b = self.coef[1,0]/2.
c = self.coef[2,0]
d = self.coef[3,0]/2.
f = self.coef[4,0]/2.
g = self.coef[5,0]

#finding center of ellipse [eqn.19 and 20] from (**)
x0 = (c*d-b*f)/(b**2.-a*c)
y0 = (a*f-b*d)/(b**2.-a*c)

#Find the semi-axes lengths [eqn. 21 and 22] from (**)
numerator = 2*(a*f*f+c*d*d+g*b*b-2*b*d*f-a*c*g)
denominator1 = (b*b-a*c)*( (c-a)*numpy.sqrt(1+4*b*b/((a-c)*(a-c)))-
(c+a))
denominator2 = (b*b-a*c)*( (a-c)*numpy.sqrt(1+4*b*b/((a-c)*(a-c)))-
(c+a))
width = numpy.sqrt(numerator/denominator1)
height = numpy.sqrt(numerator/denominator2)

# angle of counterclockwise rotation of major-axis of ellipse to x-
axis [eqn. 23] from (**)
# or [eqn. 26] from (***).
phi = .5*numpy.arctan((2.*b)/(a-c))

self._center = [x0, y0]
self._width = width
self._height = height
self._phi = phi
```

Figure 15: This is a part of the code used for fitting ellipses to the edges of the droplets. (**) refers to the site: http://mathworld.wolfram.com/Ellipse.html and (***) to A. White and B. McHale, Faraday rotation data analysis with least-squares elliptical fitting.

B.2 Appendix

```
def fit1(t, A, tau, C):
        return A*np.exp(-t/tau)+C

def fit2(p, t):
        return p[0]+p[1]*np.cos(p[2]*t+p[3]/360*np.pi)*np.exp(-t/
p[4])+p[5]*t

def errorfunc(p, t, r):
        return fit2(p,t)-r

# cutout(period number, radius, translation of data, extra data so
the set contains 597 images)
def cutout(number, r, roll, off):
    r = np.roll(r,roll)
    r = r[int(border[0 + number]):int(border[1 + number] + off)]
    return r

def fitting(number, p0, r):
    #First fitting method with std.
    b=100
    dump=np.zeros(r.size-b)

    for i in range(dump.size):
        dump[i]=np.std(r[i:i+b])

    p1=[0.60,100,0.01]
    params, pvar = scipy.optimize.curve_fit(fit1,
np.arange(dump.size), dump, p1, maxfev=100000)

    print('Fitting1')
    print(params[1]*0.001)
    print(0.001*np.sqrt(np.diag(pvar))[1])

    #Second fitting method to data directly
    pfit, pcov, infodict, errmsg, success =
scipy.optimize.leastsq(errorfunc, p0, args=(t, r), Dfun=None,
full_output=True, ftol=1e-9, xtol=1e-9, maxfev=10000000,
epsfcn=1e-10, factor=0.1)

    print('Fitting2')
    print(0.001*pfit[4])
    print(0.001*np.sqrt(np.diag(pcov))[4])
```

Figure 16: This is a a part of the code used for the fitting methods. The function fit1 is the first method where τ is fitted the data via equation (14) and function fit2 is the second method where τ is fitted to the data via equation (15).